Biochemical Journal (2019) **476** 3435–3453
https://doi.org/10.1042/BCJ20190297

PORTLAND PRESS

Research Article

The multifunctional enzyme S-adenosylhomocysteine/methylthioadenosine nucleosidase is a key metabolic enzyme in the virulence of *Salmonella enterica* var Typhimurium

Asma U. Husna[1,*], Nancy Wang[1], Jonathan J. Wilksch[1], Hayley J. Newton[1], Dianna M. Hocking[1], Iain D. Hay[2,†], Simon A. Cobbold[3], Mark R. Davies[1], Malcolm J. McConville[3], Trevor Lithgow[2] and Richard A. Strugnell[1]

[1]Department of Microbiology and Immunology, The University of Melbourne, at the Peter Doherty Institute for Infection and Immunity, Melbourne, Victoria 3000, Australia; [2]Department of Microbiology, Monash University, Clayton, Victoria 3800 Australia; [3]Department of Biochemistry and Molecular Biology, Bio21 Institute, The University of Melbourne, Parkville, Victoria 3052, Australia

Correspondence: Richard A. Strugnell (rastru@unimelb.edu.au)

Key physiological differences between bacterial and mammalian metabolism provide opportunities for the development of novel antimicrobials. We examined the role of the multifunctional enzyme S-adenosylhomocysteine/Methylthioadenosine (SAH/MTA) nucleosidase (Pfs) in the virulence of *S. enterica* var Typhimurium (*S.* Typhimurium) in mice, using a defined Pfs deletion mutant (i.e. Δ*pfs*). Pfs was essential for growth of *S.* Typhimurium in M9 minimal medium, in tissue cultured cells, and in mice. Studies to resolve which of the three known functions of Pfs were key to murine virulence suggested that downstream production of autoinducer-2, spermidine and methylthioribose were non-essential for *Salmonella* virulence in a highly sensitive murine model. Mass spectrometry revealed the accumulation of SAH in *S.* Typhimurium Δ*pfs* and complementation of the Pfs mutant with the specific SAH hydrolase from *Legionella pneumophila* reduced SAH levels, fully restored growth *ex* vivo and the virulence of *S.* Typhimurium Δ*pfs* for mice. The data suggest that Pfs may be a legitimate target for antimicrobial development, and that the key role of Pfs in bacterial virulence may be in reducing the toxic accumulation of SAH which, in turn, suppresses an undefined methyltransferase.

*Present address: DTS Food Assurance Company, Unit 3 and 5, 352 Macaulay Road Kensington, Vic 3031, Australia
†Present address: School of Biological Sciences, 3A Symonds St., Auckland, The University of Auckland, New Zealand

Received: 24 April 2019
Revised: 30 October 2019
Accepted: 1 November 2019

Accepted Manuscript online: 1 November 2019
Version of Record published: 21 November 2019

Introduction

Increasing antibiotic resistance is driving the search for novel antimicrobial drug targets and the metabolic differences between prokaryotes and eukaryotes are seen as attractive areas for target discovery [1–5]. While there is considerable overlap between eukaryotes and prokaryotes in core metabolism, there are some important differences [6–8]. The bacterial quorum-sensing systems appear to be unique and the production of the quorum-sensing molecule autoinducer-2 (AI-2) is fed by the activated methyl cycle which metabolises methionine (Met) to produce the key methyl donor S-adenosylmethionine (SAM) [9–15].

The activated methyl cycle recycles Met from SAM (Figure 1). SAM is produced from Met by the SAM synthetase (MetK) in a reaction that is essential to the bacterial cell [16–19]; enteric bacteria such as *E. coli* and *Salmonella enterica* var Typhimurium (*S.* Typhimurium) have no transporters for SAM, and null mutants of MetK are lethal in the bacteria [16,17,20]. As the methyl group is donated from SAM, demethylated SAM is produced, known as S-adenosylhomocysteine (SAH). SAH is

Biochemical Journal (2019) 476 3435–3453
https://doi.org/10.1042/BCJ20190297

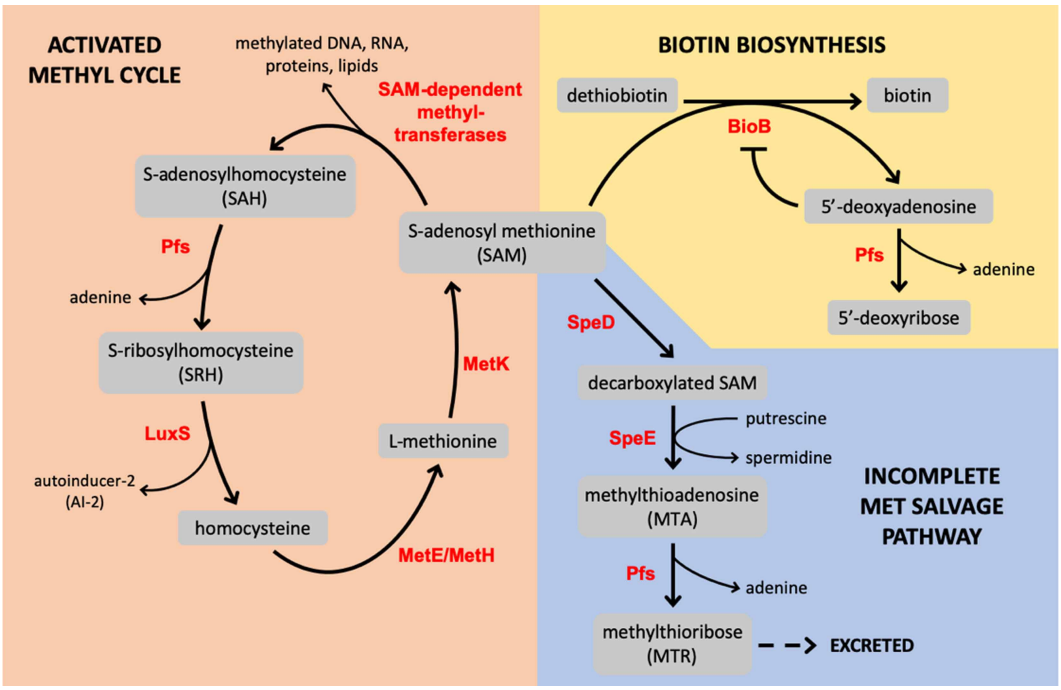

Figure 1. Activated methyl cycle, biotin biosynthesis and the incomplete Met salvage pathway in *S.* Typhimurium.
Boxes represent metabolites, enzymes are shown in red and arrows represent the direction of enzymatic reactions. MetE and MetH, partially redundant Met synthases; MetK, S-adenosylmethionine synthetase; Pfs, S-adenosylhomocysteine/methylthioadenosine nucleosidase; LuxS, S-ribosylhomocytseine lyase; SpeD, S-adenosylmethionine decarboxylase; SpeE, Spermidine synthase; BioB, biotin synthase; Pfs, S-adenosylhomocysteine/Methylthioadenosine nucleosidase; SAM, S-adenosylmethionine.

immediately converted to homocysteine and is finally recycled to Met to complete the methyl cycle. SAM is the predominant methyl donor in bacteria and is responsible for methylation of a variety of macromolecules, including DNA, by different SAM-dependent methyltransferases [18,21,22].

In *S.* Typhimurium and *E. coli,* the conversion of SAH to homocysteine is a two-step process. SAH is converted to S-ribosylhomocysteine (SRH) by SAH nucleosidase (abbreviated to Pfs) and then from SRH to homocysteine using S-ribosylhomocysteine lyase (LuxS) [23]. AI-2, an integral component of quorum sensing, is produced during the conversion of SRH to homocysteine [9–15]. AI-2 appears to function in intraspecies and interspecies communication, driven by cell density, and controls phenomena including bacterial swarming [9–15]. In eukaryotes and some bacteria, SAH is converted to homocysteine directly through a one-step process by S-adenosylhomocysteine hydrolase (SahH) [10,24,25].

Pfs has two other well-characterised enzymatic activities: it is required for the conversion of methylthioadenosine (MTA) to methylthioribose (MTR) [23], and is indirectly involved in the biosynthesis of biotin, a key vitamin, through the conversion of 5′-deoxyadenosine to 5′-deoxyribose and adenine [26,27]. The nucleoside 5′-deoxyadenonsine is an inhibitor of biotin synthase (BioB), and therefore Pfs activity indirectly affects biotin synthesis (Figure 1) [26,27].

The aim of this study was to investigate the 'essentiality' of de-methylated SAM salvage and more specifically Pfs in the virulence of *S.* Typhimurium, and to define the reason(s) why bacteria lacking Pfs were grossly attenuated in mice. Given the multiple reactions mediated by Pfs, its veracity as an antibiotic target will be defined by redundancy and the potential 'work arounds' that bacteria typically deploy to effect resistance.

Experimental procedures

Bacterial strains and growth conditions

The bacterial strains and plasmids used in this study are listed in Table 1. All mutant strains were constructed on the *S.* Typhimurium SL1344 genetic background and SL1344 was used as the wild-type strain in all

Biochemical Journal (2019) 476 3435–3453
https://doi.org/10.1042/BCJ20190297

Table 1 Strains and plasmids used for this study

Strain or plasmid	Relevant phenotypes and genotypes	Source
Strains		
Salmonella enterica Typhimurium SL1344	Wild-type strain *rpsL hisG46*; Str^R	[28]
Salmonella enterica Typhimurium BRD666	Restriction negative modification positive (r^-m^+) SL1344; Str^R	[71]
Escherichia coli DH5α	Cloning strain	[72]
Plasmids		
pGEM-T Easy	High-copy-no. cloning vector for PCR products; Ap^R	Promega
pACBSR	Medium-copy number, mutagenesis plasmid; p15A ori; Ara-inducible I-*Sce*I and λ Red recombinase; Chl^R	[29]
pACYC184	Medium-copy number cloning vector, p15A ori; Tet^R, Chl^R	[73]
pACYC184::*pfs*	*S.* Typhimurium SL1344 *pfs* cloned into pACYC184; Chl^R	This study
pACYC184::*sahH*	*L. pneumophila sahH* cloned into pACYC184; Chl^R	This study
pCP20	FLP recombinase, temperature-sensitive replicon; Ap^R, Chl^R	[74]
pKD4	FRT-flanked Km^R cassette; Ap^R, Km^R	[75]

Str, streptomycin; Ap, ampicillin; Chl, chloramphenicol; Km, kanamycin; Ara, arabinose; Flp, flippase; FRT, fippase recombinase target.

experiments. The streptomycin-resistant SL1344 strain has been described previously [28]; its virulence is well-defined. Appropriate antibiotics, including streptomycin (50 μg/ml) chloramphenicol (30 μg/ml), kanamycin (50 μg/ml) and ampicillin (100 μg/ml) were added to growth media as required. To obtain mid-exponential growth phase, *S.* Typhimurium and *E. coli* strains were grown in 10 ml Luria-Bertani (LB) broth (BD Difco) overnight, and 100 μl of the overnight culture was sub-cultured into 10 ml fresh LB broth, and grown with shaking (180 rpm) at 37°C for 3–4 h until the optical density reading at 600 nm (OD_{600}) reached 0.6–0.8. Growth phenotypes were characterised in LB broth or M9 minimal medium (2 mM $MgSO_4$, 0.1 mM $CaCl_2$, 0.4% glucose, 8.5 mM NaCl, 42 mM Na_2HPO_4, 22 mM KH_2PO_4, 18.6 mM NH_4Cl and 100 μM histidine) with or without Met or biotin supplemented as required.

For the quantitation of SAH, bacteria from overnight LB cultures were harvested by centrifugation at 4°C, and the pellets washed twice in 1× PBS before being resuspended in 1× PBS to an equivalent cell density based on OD_{600} absorbance values. A 1 in 10 dilution was used to inoculate 20 ml M9 minimal medium (supplemented with 100 μM histidine, 50 μg/ml streptomycin and, for strains carrying the pACYC184 plasmid, 30 μg/ml chloramphenicol) prior to incubation with shaking (200 rpm) at 37°C for 24 h. Five replicates of each strain were set up. The following day, the cell density of each culture was measured at OD_{600} before harvesting the bacteria as described above, cells were washed in 1× PBS and resuspended to the same cell density. Aliquots were centrifuged and the cell pellets snap-frozen in liquid nitrogen before LC–MS analysis.

For growth curves, 200 μl of M9 minimal medium (supplemented with 100 μM histidine, 100 μM Met, 50 μg/ml streptomycin and, for strains carrying the pACYC184 plasmid, 30 μg/ml chloramphenicol) was dispensed into multiple wells of a flat-bottom 96-well plate and inoculated 1 in 100 with bacterial strains of equivalent cell density that had been harvested from overnight LB cultures and washed with 1× PBS before resuspending in M9 medium. Growth was monitored for 22 h at 37°C with intermittent shaking using a FLUOstar Omega microplate reader (BMG LABTECH) set to detect absorbance at 600 nm wavelength.

Construction of strains and plasmids

Defined deletions of the sequence encoding the *pfs, speD, speE, luxS* and *bioB* genes were generated in *S.* Typhimurium SL1344. The mutant Δ*pfs* was complemented by introducing the *pfs* from *S.* Typhimurium and *sahH* gene from *Legionella pneumophila* into Δ*pfs* strain in *trans*. These strains are named as Δ*pfs* + pACYC184::*pfs* and Δ*pfs* + pACYC184::*sahH*, respectively. Gene deletions and concomitant insertions of an

Biochemical Journal (2019) **476** 3435–3453
https://doi.org/10.1042/BCJ20190297

antibiotic resistance cassette were constructed using a Lambda Red-mediated 'gene gorging' method [29]. All constructs were verified by PCR and moved to a SL1344 or relevant background via P22 phage transduction [28,30]. Primers used to construct mutants are listed in Table 2. Genetic complementation in the complemented Δ*pfs* + pACYC184::*pfs* strain was achieved by cloning *pfs* into pACYC184 via the *Bam*HI and *Sph*I sites and then introducing pACYC184::*pfs* into the Δ*pfs* mutant. Genetic complementation in the complemented Δ*pfs* + pACYC184::*sahH* strain was achieved by attaching a 3× FLAG-tag sequence at the 5′ end of *sahH*, then cloning *sahH* into pACYC184 via the *Bam*HI and *Sph*I sites and then introducing pACYC184::*sahH* into the Δ*pfs* mutant. All constructs were verified by restriction analysis and DNA sequencing. Key mutants were also sequenced using Illumina whole genome sequencing and analysed using the pipeline at the Wellcome Sanger Institute, Hinxton, U.K.

Infection of epithelial cells

Infection of HeLa cells (sourced from American Type Culture Collection (ATCC)) was conducted using established gentamicin protection assay protocols [31,32]. Briefly, HeLa cells were grown in DMEM supplemented with 10% heat-inactivated fetal calf serum (FCS) and 2 mM L-glutamax (Life Technologies), in a humidified 37°C, 5% CO_2 incubator. One day prior to infection, HeLa cells were seeded in 24-well plates at 2×10^5 cells per well. *S.* Typhimurium strains were grown to mid-exponential phase prior and frozen in LB with 10% glycerol at −80°C. Bacteria were thawed immediately before infection, washed in antibiotic-free tissue culture

Table 2 Oligonucleotide primers used in this study for construction of mutants and complementation

Mutants	Sequence (5′–3′)
Δ*pfs*-ISceI-F	TAGGGATAACAGGGTAATGAAACCACACAGCGATCATG
Δ*pfs*-ISceI-R	TAGGGATAACAGGGTAATGGTAAACAGAGGATTCATGCC
Δ*pfs*–Kan-F	**CTAAGGAGGATATTCATATG**GAAACAGTCGACTCTGATGGTC
Δ*pfs*-Kan-R	**GAAGCAGCTCCAGCCTACACA**CCGTTCAACTGGCCAGTG
Δ*speD*-ISceI-F	**TAGGGATAACAGGGTAATCGCGCTTTACGCTGGTAAT**
Δ*speD*-ISceI-R	TAGGGATAACAGGGTAATCTGGATGCCGGTACGACAAT
Δ*speD*-Kan-F	**CTAAGGAGGATATTCATATG**GATGCGCGAGATTTACTACGG
Δ*speD*-Kan-R	**GAAGCAGCTCCAGCCTACACA**GCTCTTCTGCGGTTTTGGC
Δ*speE*-ISceI-F	TAGGGATAACAGGGTAATGTCGCTACGTTCTCAGTATGC
Δ*speE*-ISceI-R	TAGGGATAACAGGGTAATGAACGTTGTCTACGGCAAAG
Δ*speE*-Kan-F	**CTAAGGAGGATATTCATATG**GCTATTACAACCCGGCTATTC
Δ*speE*-Kan-R	**GAAGCAGCTCCAGCCTACACA**GAACGTTGTCTACGGCAAAG
Δ*luxS*-ISceI-F	TAGGGATAACAGGGTAATGACGTTAGGCATTGGCTGTG
Δ*luxS*-ISceI-R	TAGGGATAACAGGGTAATCTGCTGCTGTTTCAACGAGC
Δ*luxS*–Kan-F	**CTAAGGAGGATATTCATATG**CGTCATATTCTGGAGCGTGA
Δ*luxS*-Kan-R	**GAAGCAGCTCCAGCCTACACACA**GATCAAACACGGTGATTGC
Δ*bioB*-ISceI-F	TAGGGATAACAGGGTAATGAACGTGTCGCCATGATAACC
Δ*bioB*-ISceI-R	TAGGGATAACAGGGTAATCTGTCACCACCAGTTGCTGAC
Δ*bioB*-Kan-F	**CTAAGGAGGATATTCATATG**GGCAGAGGACAAGGATCTGC
Δ*bioB*-Kan-R	**GAAGCAGCTCCAGCCTACACA**CTGGCGATGAATTTGCTGC
pfs-BamH1-F	TGGATCCCTCATGCTCCGTCTTTACACC
pfs-Sph1-R	TGCATGCGAATAGCTGCTGACGCCAAC
sahH-BamH1-F	TGGATCCATGGACTACAAAGACCATGACGGTGATTATAAAGATCATGACATCGATTACAAGGATGACGATGACAAGATGGAACTGGTAG AAGAAGGAG
sahH-Sph1-R	TGCATGCGATTTAGTTATCTTGACTAAATC

Endonuclease restriction sites are underlined; kanamycin^R-cassette specific sequences are in bold; F, forward (5′) primer; R, reverse (3′) primer.

media and diluted in DMEM media with or without L-Met, then added to HeLa cell monolayers at a multiplicity of infection (MOI) of 5–10. The colony-forming units (cfu) in the inoculum were estimated by plating on LB agar plates. Infected HeLa cells were centrifuged at 600×*g* for 5 min immediately after the addition of bacteria and then incubated for 1 h at 37°C. After 1 h, the tissue culture media was replaced with DMEM media with or without Met and containing 100 μg/ml of gentamicin to kill extracellular bacteria. The concentration of gentamicin was reduced to 10 μg/ml at 2 h post-infection and maintained for the remainder of the experiment. To enumerate intracellular bacteria, cells were washed twice with PBS, and lysed with 1% Triton X-100 (Sigma) for 15 min to release the intracellular bacteria. The bacteria were enumerated by plating appropriate dilutions on LB agar plates.

Ethics statement

All animal research conducted in this study was approved by the Animal Ethics Committee (Biochemistry & Molecular Biology, Dental Science, Medicine, Microbiology & Immunology) at The University of Melbourne, under project number 1413141. All experiments were conducted in accordance with the Australian Code of Practice for the Care and Use of Animals for Scientific Purposes, 8th edition 2013.

Mouse infections

All animal experiments were carried out at the Biological Research Facility (BRF) at the Department of Microbiology and Immunology, The University of Melbourne, at Peter Doherty Institute for Infection and Immunity. Age- and sex-matched C57BL/6 mice were used between 6–8 weeks of age and all 144 mice used as sources of data in this manuscript were euthanased prior to isolation of infected tissues.. To assess the virulence of mutant strains, either the intravenous or oral route of infection was used. For intravenous infections, 200 cfu of each bacterial strain was prepared in 200 μl PBS and injected into the lateral tail vein. For oral infections, mice were orally gavaged with 100 μl 10% sodium bicarbonate immediately before oral gavage of 100 μl containing ∼5 × 107 cfu of S. Typhimurium strains. To prepare the inoculum, all strains of S. Typhimurium were grown shaking at 180 rpm in M9 minimal medium (for S. Typhimurium Δpfs mutant the M9 medium was supplemented with 100 μM Met and 100 μM biotin) at 37°C for 24 h, and stored in 10% glycerol at −80°C until use. Immediately prior to infection, the stored aliquots were thawed and diluted in PBS to the required concentration. At designated time points post-infection, the spleen and liver were removed aseptically, homogenised using the Stomacher 80 Biomaster paddle blender (Seward), and serial dilutions were plated on LB agar plates with 50 μg/ml streptomycin to determine the bacterial load.

Western blot analysis

The expression of 3×FLAG*SahH* (from pACYC184::*sahH*) was detected by Western blot analysis using a monoclonal mouse Anti-FLAG antibody (Sigma) at a concentration of 1 : 2000. *S.* Typhimurium whole-cell lysates were prepared from overnight cultures. Samples were separated by sodium dodecyl Sulfate (SDS)-polyacrylamide gel electrophoresis (PAGE) and transferred to iBlot2 NC Regular stack nitrocellulose (Thermo Fisher Scientific) using an iBlot2 Gel Transfer Driver (Life technologies, CA) at 20 V for 6–7 min. The membrane was blocked for 1 h at 25°C in rotating condition using blocking buffer. The primary antibody was diluted 1 : 2000 in blocking buffer and incubated with the membrane at 4°C overnight under rotating condition. The membrane was washed with 0.05% skim-milk in Tween-20 3 times, 10 min each, under rotating condition. Anti-mouse antibody conjugated with Horseradish Peroxidase (HRP) (Bio-Rad) was used as the secondary antibody at a concentration of 1 : 10 000 in blocking buffer and the membrane was incubated under rotating condition for 1 h at 25°C. The membrane was then washed with 0.05% skim-milk in Tween-20 three times, 10 min each, under rotating condition. Bound antibody was visualised with ECL Western Blotting Detection Reagents used according to the manufacturer's instructions (Amersham Biosciences). The development step occurred typically within 2–3 min and the membrane was imaged by using DNR-Bioimaging System (MF-ChemiBis 3.2).

Mass spectrometry analysis

Cell pellets were thawed and metabolites were extracted with 125 μl of 80% acetonitrile and briefly vortexed. Samples were centrifuged for 10 min at 14 000×*g* and the supernatant transferred to glass vials for LC–MS analysis. SAM was detected on an Agilent 6545b using a zic-pHILIC column (150 × 4.6 mm, Merck) as previously described [33]. Briefly, data was acquired in full scan mode (60–1200 m/z), and the retention time of SAM was

Biochemical Journal (2019) 476 3435–3453
https://doi.org/10.1042/BCJ20190297

confirmed with a synthetic standard (Sigma). All features were extracted in the MAVEN software package [34] prior to file conversion with MSConvert. Samples were median normalised and the SAM integrated peak was plotted using GraphPad Prism.

Sequence similarity network analysis

Sequence similarity network analysis: representative protein sequences for MTA/SAH nucleosidase (InterPro family IPR010049 – 3240 sequences) and Adenosylhomocysteinase (InterPro family IPR034373 – 4657 sequences) were extracted from the uniref90 database. All sequences were used as a database to perform an all-against-all pairwise BLAST and a sequence similarity network was generated and assessed with CLANS [35] with E-value cut off as described in the figure legend.

DNA methylation analysis

Strains were grown for 24 h in M9 minimal medium supplemented with Met and appropriate antibiotics. Cells were incubated in lysis buffer (10 mM Tris pH 8.0 containing 0.38% SDS, 2 mg/ml lysozyme, 0.9 mg/ml Proteinase K, and 200 μg/ml RNase A) for 30 min at 37°C, followed by 30 min at 55°C. Genomic DNA was extracted with phenol/chloroform using 5PRIME Phase Lock Gel light tubes (Quantabio), precipitated with 3 M sodium acetate and isopropanol, then washed with 70% (v/v) ethanol. DNA concentration was measured using a NanoDrop 2000 spectrophotometer and visualised after gel electrophoresis through a 0.6% (w/v) agarose gel stained with SYBR Safe DNA gel stain (Invitrogen). Detection of DNA methylation in the form of 5-methylcytosine (5-mC) was performed using the MethylFlash Global DNA Methylation (5-mC) ELISA colorimetric kit as per the manufacturer's instructions (Epigentek). Duplicate samples (100 ng/well) of each biological replicate were screened in the assay and the absorbance read at OD_{450} using a FLUOstar Omega microplate reader. Percentage of 5-mC DNA in total DNA was calculated after determining the slope of the standard curve using linear regression and the formula: (sample OD − neg control OD)/(slope × 100 ng) × 100%. The presence of *dam* methylation was assessed by digestion of 1 μg genomic DNA overnight at 37°C with restriction enzymes *Dpn*I, *Dpn*II and *Mbo*I, and methylation non-sensitive restriction enzyme Sau3A as per manufacturer's instructions (NEB). Digested DNA was visualised using gel electrophoresis, as described above, and imaged with the Syngene G:BOX gel documentation system.

Results

S. Typhimurium Δ*pfs* mutant is highly attenuated in mice

A Pfs mutant of virulent *S.* Typhimurium SL1344 was constructed by allelic exchange and the mutant was sequenced. The role of Pfs in the virulence of *S.* Typhimurium was examined by testing the growth of the mutant in C57BL/6 mice, and growth was compared with that of the wild-type SL1344 (Figure 2). There was 10 000-fold less *S.* Typhimurium Δ*pfs* recovered from the spleen or liver of infected mice, compared with wild-type SL1344; complementation with *pfs* on pACYC184 restored *in vivo* growth of the bacterium to wild-type levels. C57BL/6 mice were also orally infected with 5×10^7 cfu of SL1344 or the Δ*pfs* mutant (Supplementary Figure S1). The mice were euthanised on day 6 post-infection, the spleen and liver was removed, and the number of bacteria was enumerated by viable count. Again, 10 000-fold less *S.* Typhimurium Δ*pfs* were recovered compared with SL1344.

These data indicate that MTA/SAH nucleosidase (Pfs) is essential for the replication of *S.* Typhimurium in the C57BL/6 mouse, which is known to be highly sensitive to infection [36]. To explore why this attenuation occurred, *S.* Typhimurium Δ*pfs* was investigated for *in vitro* growth characteristics.

S. Typhimurium Δ*pfs* is an auxotroph requiring biotin or Met for growth under minimal nutrient conditions

The metabolic phenotype of the *S.* Typhimurium Δ*pfs* mutant was determined in M9 minimal medium. *S.* Typhimurium Δ*pfs* was unable to grow in M9 minimal medium (Figure 3A), but replicated in nutrient-rich LB medium (Figure 3B), suggesting that the Δ*pfs* mutant is an auxotroph that requires additional nutrients to grow under the nutrient restrictions imposed by M9 medium. To confirm that the deleted *pfs* gene was responsible for auxotrophy, the replication of *S.* Typhimurium Δ*pfs* + pACYC184::*pfs* in M9 minimal medium and LB medium was assessed (Figure 3A,B). This complemented strain grew in M9 minimal medium at levels

Biochemical Journal (2019) **476** 3435–3453
https://doi.org/10.1042/BCJ20190297

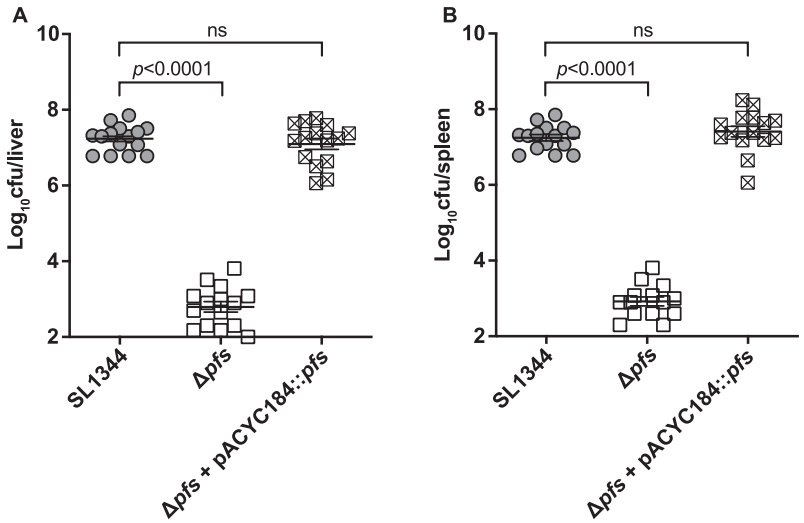

Figure 2. *S.* Typhimurium lacking Pfs is severely attenuated in mice.

C57BL/6 mice were i.v. infected with 200 cfu of wild-type *S.* Typhimurium SL1344 or the Δ*pfs* mutant. On day 5 post-infection, (**A**) the liver and (**B**) spleen were harvested to determine the bacterial load in the organs. Symbols represent data from individual animals, and horizontal lines represent the geometric mean of each group. Error bars represent the standard error of the mean (SEM). Data are pooled from three independent experiments. One-way ANOVA with Bonferroni post-test was used for statistical tests; ns = not significant ($P > 0.05$).

comparable to the wild-type, demonstrating that the growth restored in the mutant was dependent on the presence of a functional Pfs.

To further characterise the specificity of auxotrophy in *S.* Typhimurium Δ*pfs*, the bacterium was grown in M9 media supplemented with either 100 μM Met or 100 μM biotin. Supplementation of either Met or biotin supported the growth of the Δ*pfs* mutant at near wild-type levels in M9 (Figure 3C). The study was expanded by titrating the effects of biotin and Met on growth. *S.* Typhimurium Δ*pfs* grew to similar levels as SL1344, albeit at a slower growth rate over 60 h, in M9 minimal medium that contained reducing levels of biotin and Met, and down to 0.1 μM of either (Figure 3C). To test whether the attenuation seen in mice was reflected by reduced intracellular growth in tissue culture cells, the Pfs mutant was used to infect HeLa cells (Figure 3D). Again, growth attenuation was observed, which was restored when the Pfs mutant was complemented with pACYC184 carrying *pfs*. Given that Met could reverse the auxotrophy observed in M9 medium, the growth in HeLa cells of *S.* Typhimurium Δ*pfs* was compared with mutants unable to both synthesise Met *de novo*, through deletion of *metB*, or by mutating the two Met synthases (MetE and MetH), and transport Met through the high-affinity transporter which consists of MetN, MetI and MetQ [37]. These bacteria that were deficient in Met import and *de novo* synthesis grew intracellularly in HeLa cells (Figure 3D), unlike *S.* Typhimurium Δ*pfs*, which replicated only very slowly inside cells (Figure 3). These data suggest that the growth attenuation observed for *S.* Typhimurium Δ*pfs* in HeLa cells was not due to a Met auxotrophy, but might have been due to suppression of biotin synthesis by accumulating 5′-deoxyadenosine.

To test whether a BioB mutation phenocopied *S.* Typhimurium Δ*pfs*, a defined mutant was constructed and tested in M9 minimal medium, for growth in HelLa cells, and for virulence in mice. *S.* Typhimurium Δ*bioB* was an auxotroph in M9 (Figure 4A), that was reversed by the addition of biotin (Figure 4B). *S.* Typhimurium Δ*bioB* was able to grow in HeLa cells (Figure 4C) and was at least as virulent as *S.* Typhimurium SL1344 when mice were infected i.v., measured by growth of the *S.* Typhimurium Δ*bioB* in the liver or spleen of infected mice, examined 5 days post-infection (Figure 4D,E, respectively).

S. Typhimurium Δ*speD*, Δ*speE* and Δ*luxS* mutants are not attenuated for growth in HeLa cells or in mice

We next aimed to determine why *S.* Typhimurium Δ*pfs* was attenuated *in vivo*. Given *S.* Typhimurium with mutations in *de novo* Met biosynthetic pathways showed normal growth and virulence in mice [37], the

Biochemical Journal (2019) 476 3435–3453
https://doi.org/10.1042/BCJ20190297

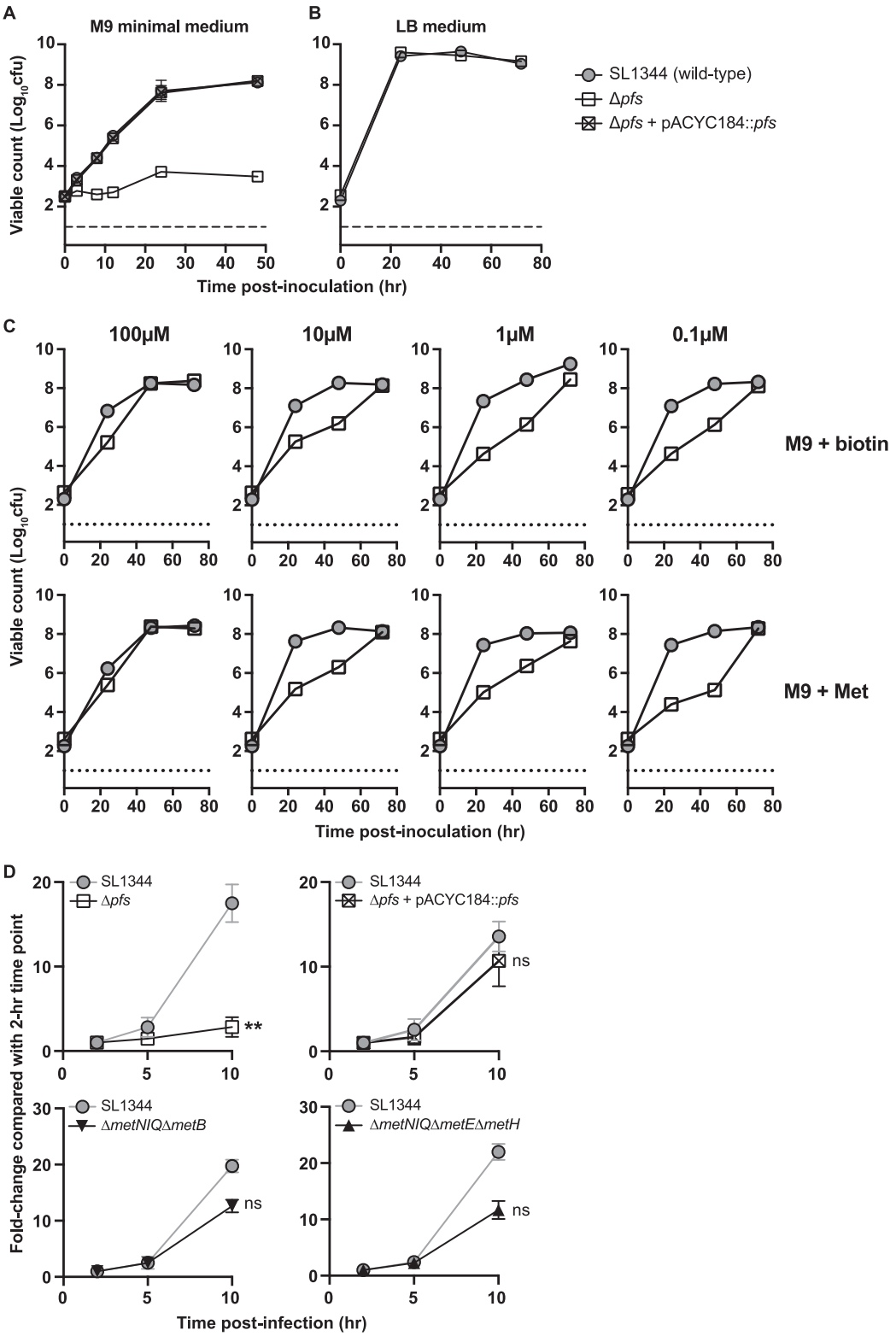

Figure 3. *S.* Typhimurium Δ*pfs* mutant is unable to grow in M9 minimal medium and is attenuated for intracellular growth in HeLa cells. Part 1 of 2

(**A**) M9 minimal medium, (**B**) LB nutrient medium, or (**C**) M9 minimal media supplemented with indicated concentration of biotin or Met was inoculated with 200 cfu of *S.* Typhimurium wild-type SL1344 or Δ*pfs* mutant, and grown aerobically at 37°C.

Biochemical Journal (2019) **476** 3435–3453
https://doi.org/10.1042/BCJ20190297

Figure 3. *S.* Typhimurium Δ*pfs* mutant is unable to grow in M9 minimal medium and is attenuated for intracellular growth in HeLa cells. Part 2 of 2

The viable bacterial count was determined at indicated time points. Horizontal bars represent the geometric mean of each group, and error bars represent the standard deviation (SD). Dotted lines represent the detection limit for bacterial concentration. Data are pooled from two independent experiments. D) *S.* Typhimurium wild-type and mutant strains were tested for intracellular replication in HeLa cells. HeLa cells were grown to a monolayer and infected with *S.* Typhimurium wild-type or mutant strains at a multiplicity of infection (MOI) of 5–10, in complete DMEM. The intracellular bacterial load at 2 h post-infection is expressed as '1' and used as the reference point to calculate fold-change of intracellular bacterial number at subsequent time points. Data are pooled from three independent experiments. Bars represent the mean fold-change and error bars show the SD. Unpaired *t*-tests were used to compare the intracellular load of wild-type and mutant strains at 10 hr post-infection, and *P*-values shown were corrected for multiple comparisons using the Bonferroni-Dunn method; ** indicates $P < 0.01$, and *P*-values greater than 0.05 were deemed as not significant (ns).

apparent auxotrophy for Met, as was observed in M9 minimal medium, does not readily explain why *S.* Typhimurium Δ*pfs* was highly attenuated in mice. Therefore, further mutants were constructed to determine if the attenuation in Δ*pfs* was due to either deficiency of downstream metabolites, such as the polyamine, spermidine, or AI-2. To test this, we generated mutants carrying defined deletions in *speD* and *speE*, responsible for spermidine biosynthesis, and *luxS*, the S-ribosylhomocysteine lyase that produces the quorum sensing ligand, AI-2 (Figure 1).

The three mutants were grown in M9 minimal medium and none displayed growth characteristics that were different from the wild-type (Figure 5A). The Δ*pfs* mutant was also tested for swarming and the swarming phenotype was severely reduced with the deletion of Pfs, to levels equal to that observed in a non-flagellated mutant (Supplementary Figure S2). As expected, the Δ*LuxS* mutant also showed an swarming deficiency (data not shown). To determine whether *S.* Typhimurium Δ*speD*, Δ*speE* and Δ*luxS* mutants grew in mammalian cells, HeLa cells were infected with bacterial strains and the number of intracellular bacteria determined over a 10-hr period. All three mutant strains (Δ*speD*, Δ*speE* and Δ*luxS*) grew at similar rates to the wild-type in HeLa cells (Figure 5B). We then examined the role of SpeD, SpeE and LuxS enzymes in the virulence of *S.* Typhimurium in C57BL/6 mice. Mice were i.v. infected with 200 cfu of *S.* Typhimurium wild-type or mutant strains, and the bacterial load in the spleen and liver was determined at day 5 post-infection. There was no significant difference in the number of bacteria recovered from the spleen or liver of mice infected with Δ*speD*, Δ*speE* and Δ*luxS* when compared with the bacterial burden found in the organs of mice infected with wild-type SL1344 (Figure 5C,D). This result indicates that the enzymes SpeD, SpeE and LuxS are not essential for growth of *S.* Typhimurium in C57BL/6 mice, and that the *in vivo* growth attenuation observed in *S.* Typhimurium Δ*pfs* is unlikely to be due to loss of AI-2 (LuxS) or spermidine, the precursor of spermidine, decarboxylated SAM, or MTA. These data do not rule out growth attenuation through the accumulation of MTA or SAH.

The removal of S-adenosylhomocysteine (SAH) from the *S.* Typhimurium Δ*pfs* mutant restores virulence

In *E. coli* and *Salmonella*, the conversion of SAH to homocysteine is a two-step process that occurs via S-ribosylhomocysteine (SRH) [23]. SAH, through Pfs, is converted to SRH, and SRH is converted into homocysteine via LuxS, liberating the quorum sensing AI-2 [9–15,23] (Figure 1). The activated methyl cycle is reinitiated when Met is synthesised from homocysteine by one or both Met synthases [23]. In many eukaryotes and some prokaryotes, such as *Legionella pneumophila*, this cycle is different, and SAH is converted directly to homocysteine through S-adenosylhomocysteine hydrolase (SahH) [10,24,25]. Previous reports suggest that SAH is a potent inhibitor of SAM-dependent methyltransferase [38–40]. Hence, we hypothesised that the heterologous expression of an exogenous SAH hydrolase (i.e. SahH) in *S.* Typhimurium Δ*pfs*, might resolve whether the accumulation of the putatively inhibitory metabolite (i.e. SAH) was important in the attenuation of the Δ*pfs* mutant, as SahH restores only one of the three enzymatic functions of Pfs. To test this hypothesis, *S.* Typhimurium Δ*pfs* + pACYC184::*sahH* was constructed expressing SahH from *Legionella pneumophila* and expression of the *Legionella* enzyme confirmed by Western blot (Figure 6A). *Legionella* SahH does not have significant protein sequence homology with the enterobacterial Pfs and is of a different length, and similar to the human enzyme (Supplementary Figure S3).

Biochemical Journal (2019) **476** 3435–3453
https://doi.org/10.1042/BCJ20190297

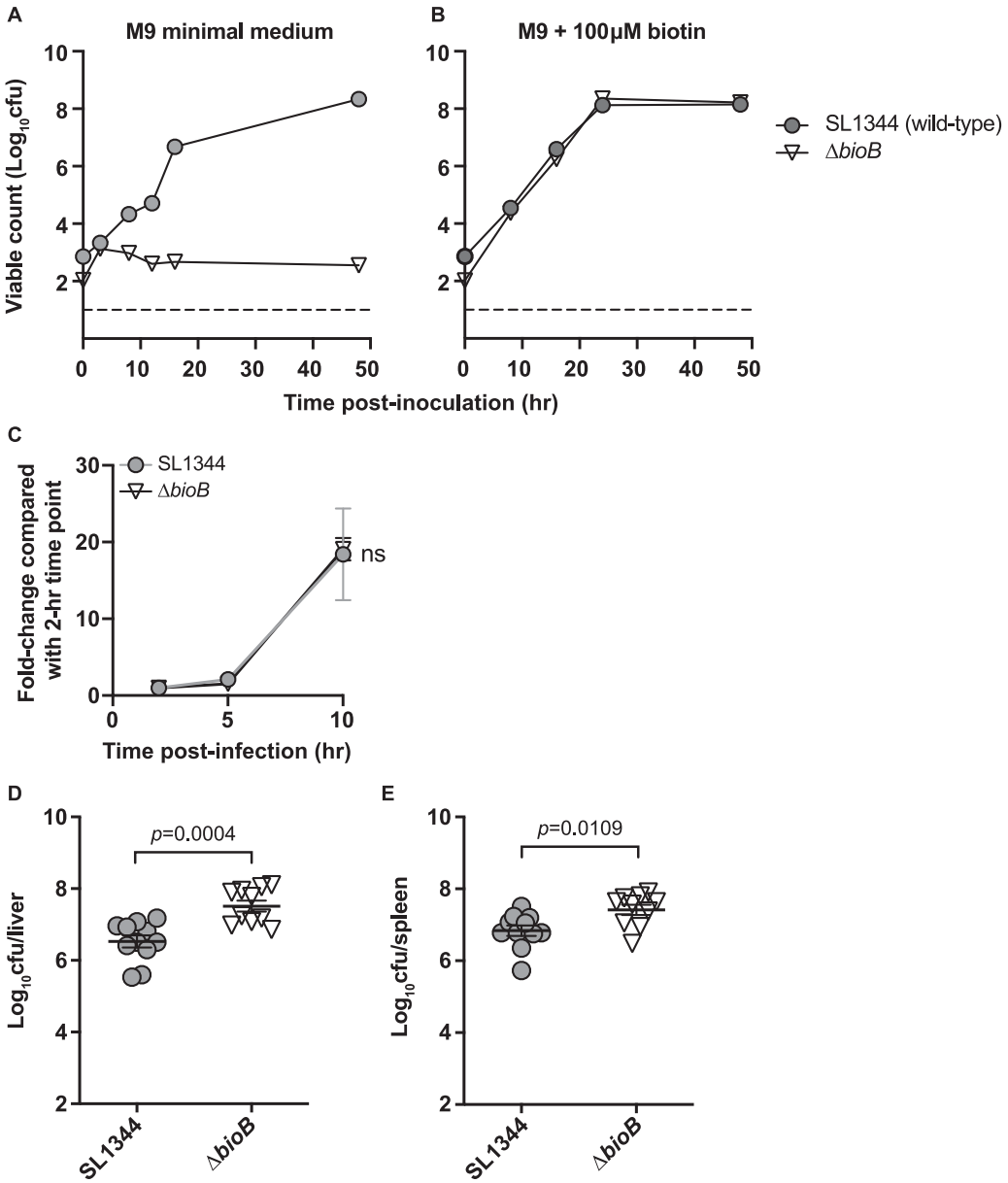

Figure 4. The *S.* Typhimurium Δ*bioB* mutant is a biotin auxotroph that shows normal growth in HeLa cells, and is fully virulent in mice.

(**A**) *S.* Typhimurium Δ*bioB* was unable to grow in M9 minimal medium without biotin supplementation. (**B**) The growth of *S.* Typhimurium in M9 was restored with addition of 100 μM biotin. Geometric mean ± SD is shown. Dotted lines represent the detection limit for bacterial concentration. Data are pooled from two independent experiments. (**C**) *S.* Typhimurium Δ*bioB* grew to similar levels as wild-type SL1344 over a 10-h period in HeLa cells, as described for Figure 3. Data are pooled from three independent experiments. Bars represent the mean fold-change and error bars show the SD. Unpaired *t*-test was used to compare the intracellular load of wild-type and mutant strains at 10 h post-infection; *P*-values greater than 0.05 were deemed as not significant (ns). For assessing virulence *in vivo*, age- and sex-matched C57BL/6 mice were i.v. infected with 200 cfu of indicated strains of *S.* Typhimurium, and the bacterial load in the (**D**) liver and (**E**) spleen was determined at day 5 post-infection. Symbols represent data from individual animals, and the geometric mean ± SEM is shown. Data are pooled from two independent experiments. The unpaired *t*-test was used for statistical analyses.

Biochemical Journal (2019) **476** 3435–3453
https://doi.org/10.1042/BCJ20190297

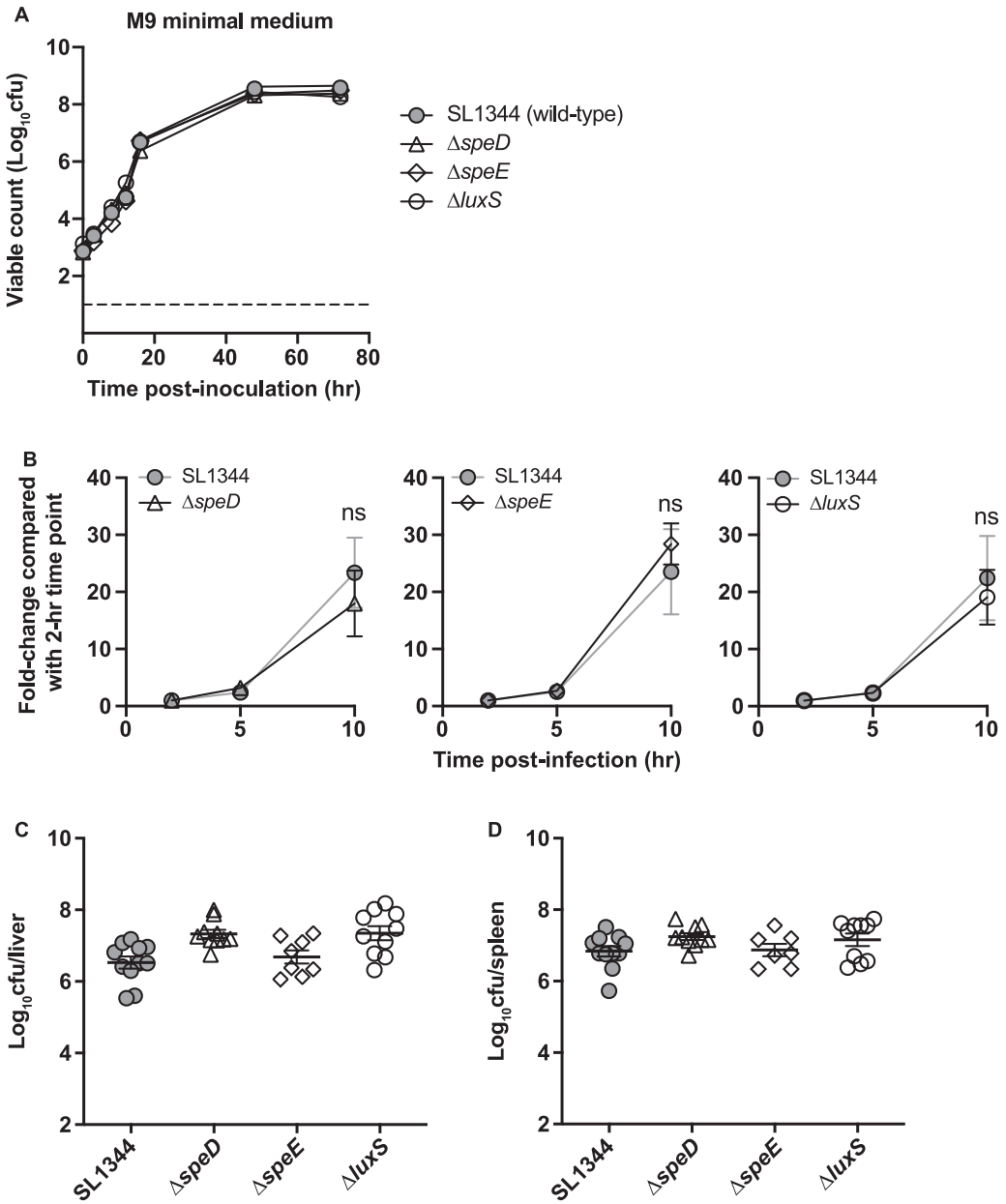

Figure 5. The *S.* Typhimurium Δ*speD*, Δ*speE* and Δ*luxS* mutants show no auxotrophy in M9 minimal medium, grow normally in HeLa cells, and are fully virulent in mice.

(**A**) *S.* Typhimurium Δ*speD*, Δ*speE* and Δ*luxS* mutants grew in M9 minimal medium without additional supplementation. Geometric mean ± SD is shown. Dotted lines represent the detection limit for bacterial concentration. Data were pooled from two independent experiments. (**B**) *S.* Typhimurium Δ*speD*, Δ*speE* and Δ*luxS* grew to similar levels as wild-type SL1344 over a 10-h period in HeLa cells, as described for Figure 3. Data are pooled from three independent experiments. Bars represent the mean fold-change and error bars show the SD. Unpaired *t*-tests were used to compare the intracellular load of wild-type and mutant strains at 10 h post-infection; *P*-values greater than 0.05 were deemed as not significant (ns). For assessing virulence *in vivo*, age- and sex-matched C57BL/6 mice were i.v. infected with 200 cfu of indicated strains of *S.* Typhimurium, and the bacterial load in the (**C**) liver and (**D**) spleen was determined at day 5 post-infection. Symbols represent data from individual animals, and the geometric mean ± SEM is shown. Data are pooled from two independent experiments.

Biochemical Journal (2019) **476** 3435–3453
https://doi.org/10.1042/BCJ20190297

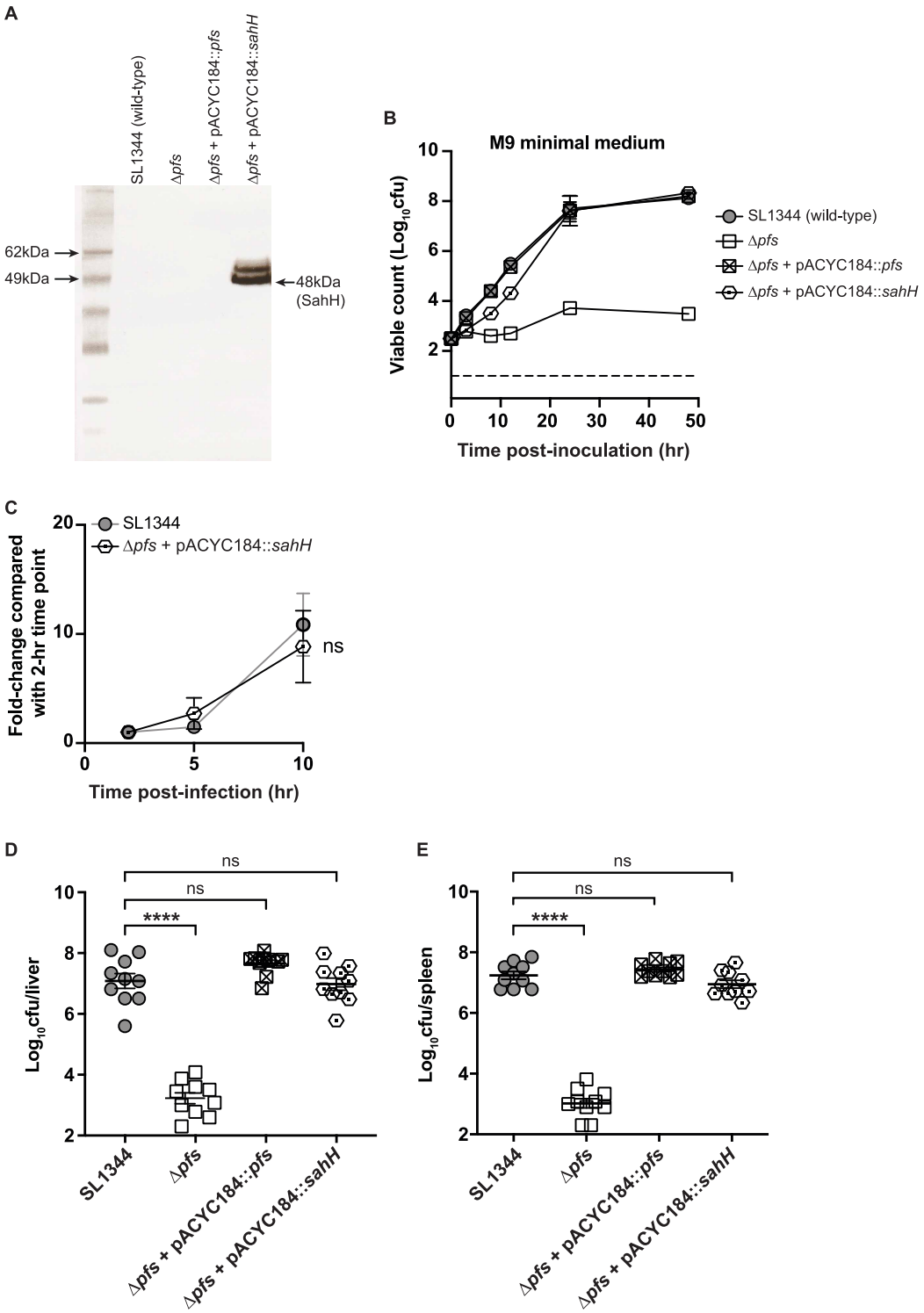

Figure 6. The SahH from *Legionella pneumophila* reverts the M9 auxotrophy of the *S.* Typhimurium Δ*pfs* mutant and growth in HeLa cells, and restores virulence in mice. Part 1 of 2

The gene encoding SahH from *Legionella pneumophila* was isolated by PCR and ligated to pACYC184 to generate pACYC184::*sahH*. The SahH produced carried a FLAG tag at the amino-terminus This plasmid was used to complement *S.* Typhimurium Δ*pfs* and complementation was compared with that achieved by pACYC194::*pfs*, i.e. the *pfs* from *S.* Typhimurium. (**A**) Western blot revealed the heterologous expression of SahH in *S.* Typhimurium Δ*pfs* mutant complemented with the *sahH* gene (Δ*pfs* + pACYC184::*sahH*) from *Legionella pneumophila*. Cell pellets were collected from 1ml of bacterial

Figure 6. The SahH from *Legionella pneumophila* reverts the M9 auxotrophy of the *S.* Typhimurium Δ*pfs* mutant and growth in HeLa cells, and restores virulence in mice. Part 2 of 2

culture grown in M9 minimal meidum supplemented with Met (100 μM) and biotin (100 μM). The Western blot was probed using antisera to the FLAG tag attached to SahH. SahH is predicted to be a 48 KDa protein. (**B**) The auxotrophic phenotype of *S.* Typhimurium Δ*pfs* in M9 medium (without Met or biotin supplementation) was reverted by complementation with the SahH enzyme. Geometric mean ± SD is shown. Dotted lines represent the detection limit for bacterial concentration. Data were pooled from two independent experiments. (**C**) Δ*pfs* + pACYC184::*SahH* grew to similar levels as wild-type SL1344 over a 10-h period in HeLa cells, as described for Figure 3. Data are pooled from three independent experiments. Bars represent the mean fold-change and error bars show the SD. Unpaired *t*-test was used to compare the intracellular load of wild-type and mutant strains at 10 h post-infection; *P*-values greater than 0.05 were deemed as not significant (ns). For assessing virulence *in vivo*, age- and sex-matched C57BL/6 mice were i.v. infected with 200 cfu of indicated strains of *S.* Typhimurium, and the bacterial load in the (**D**) liver and (**E**) spleen was determined at day 5 post-infection. Symbols represent data from individual animals, and the geometric mean ± SEM is shown. Data are pooled from two independent experiments. One-way ANOVA with Bonferroni's post-test was used for statistical analyses, **** indicates $P < 0.0001$, and *P*-values greater than 0.05 were deemed as not significant (ns).

The growth of *S.* Typhimurium Δ*pfs* + pACYC184::*sahH* in M9 minimal medium was compared with that of the Δ*pfs* mutant, the homologous complemented strain Δ*pfs* + pACYC184::*pfs* and wild-type SL1344 in M9 medium. Growth by *S.* Typhimurium Δ*pfs* in M9 medium was restored by the heterologous complementation and the Δ*pfs* mutant expressing *Legionella* SahH grew to a similar level to the wild-type SL1344 (Figure 6B). Similarly in HeLa cells, the growth reduction seen in *S.* Typhimurium Δ*pfs* (e.g. Figure 3D) was abolished by

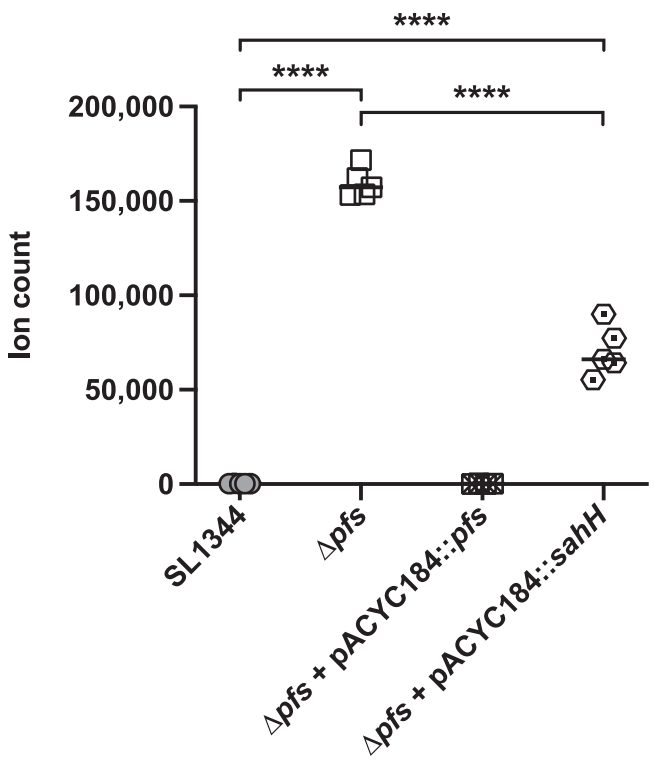

Figure 7. LC–MS/MS analysis of SAH levels show *SahH* complementation reduces SAH accumulation in the absence of Pfs.

S. Typhimurium strains were grown overnight in LB broth, washed then sub-cultured into M9 minimal medium for 24 h. The cells were pelleted, then snap frozen before analysis by mass spectrometry for levels of SAH, determined by ion count at the relevant mass. A SAH standard was used to validate the mass (data not shown). The statistical analysis was conducted using a one-way ANOVA with Bonferroni's post-test.

Biochemical Journal (2019) 476 3435–3453
https://doi.org/10.1042/BCJ20190297

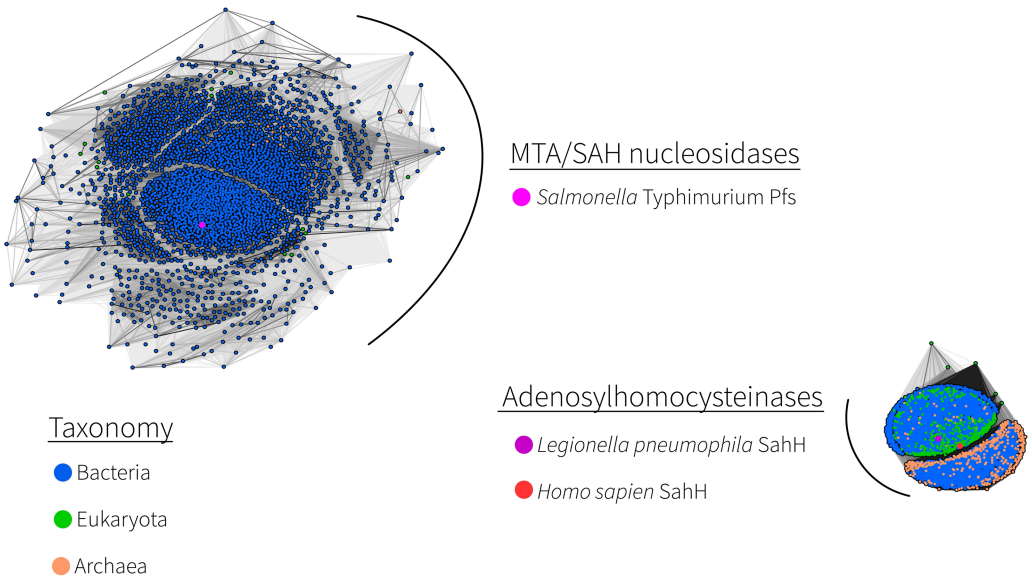

Figure 8. Similarity Network Analysis of bacterial MTA/SAH nucleosidases.

Sequence similarity network analysis of the MTA/SAH nucleosidase (Pfs) and Adenosylhomocysteinase (SahH) protein families. Each dot represents one Uniref90 sequence cluster with the gray lines between them with the most similar sequences shown as black and less similar in grey, with an E-value cutoff of 1×10^{-20}. This analysis shows two distinct unrelated protein families. The taxonomic lineage — Eukaryota (green), Archaea (orange), and Bacteria (blue) are shown. The uniref90 sequences for *Salmonella* Pfs (Unirfe90_A9MPK2), *Legionella* SahH (Uniref90_Q5WV19) and Human SahH (Uniref90_P23526) are coloured as shown in the figure text.

complementation with pACYC184::*sahH*, which restored growth of the Pfs mutant in HeLa cells to wild-type levels (Figure 6C). Lastly, the capacity of *S.* Typhimurium Δ*pfs* + pACYC184::*sahH* to grow in mice was examined. On day 5 post-infection, the bacterial burden in the spleen and liver showed that complementation with the *sahH* gene in *S.* Typhimurium Δ*pfs* fully restored growth in the mice (Figure 6D,E). This result suggests that the accumulation of SAH was likely the cause of *in vivo* attenuation in the Δ*pfs* mutant.

The levels of SAH in the different bacterial strains were analysed by mass spectrometry (Figure 7). Wild-type *S.* Typhimurium SL1344 contained undetectable levels of SAH, in contrast with *S.* Typhimurium Δ*pfs* which had much higher levels of SAH, measured as ion count by LC–MS. There was no accumulation of SAH Δ*pfs* + pACYC184::*pfs*, and the levels of SAH were reduced by 60% in the Δ*pfs* strain complemented with pACYC184::*sahH*. To determine whether this accumulation of SAH was coincident with changes in DNA methylation, the level of DNA methylation in each of the mutants was examined using two methods. Firstly, genomic DNA was extracted from the strains and analysed using antibody specific for methylated DNA (Supplementary Table S1). In addition, DNA samples were subjected to digestion by nucleases that are either methylation dependent, or inhibited by methylation (Supplementary Figure S4). The DNA methylation patterns were not different in the Pfs mutant compared with SL1344, when tested by either method.

Lastly, in order to analyse the relatedness of the bacterial Pfs and eukaryotic SahH enzymes, a Similarity Network Analysis was undertaken using libraries of prokaryotic and eukaryotic protein sequences. The output of the analysis is shown in Figure 8. The analysis reveals that, amongst the Pfs enzymes (MTA/SAH nucleosidases), there are 3–4 subgroupings, but these sequences are inherently different from the SahH enzymes that include some bacteria (e.g. *Legionella pneumophila)* as well as Archaea and indeed human SahH. These quite different clusterings of sequences suggest separate evolution of the Pfs family of enzymes from the SahH family.

Discussion

It has been posited that Pfs, a multifunctional bacterial enzyme, might provide a target for novel antimicrobial development [22]. Pfs has multiple enzymatic roles which include, directly or indirectly, controlling the levels

of a key vitamin, biotin, the detoxification of SAH and the production of a substrate for production of AI-2, and Met and adenine recycling [9–15,22,23,26,27]. We examined the virulence of a *S.* Typhimurium deletion mutant of *pfs*, and demonstrated auxotrophy in M9 minimal medium, a lack of intracellular growth in HeLa cells, and a very high degree of growth attenuation in C57BL/6 mice, a highly stringent murine challenge model.

As the enzyme description suggests, the MTA/SAH nucleosidase encoded by *pfs*, which is present in many bacteria including *E. coli* and *Salmonella*, is multifunctional. Pfs catalyses the conversion of SAH to SRH, mediates the hydrolysis of 5-MTA to 5-MTR and adenine, and converts 5′deoxyadenosine to 5′deoxyribose and adenine [23,41,42]. Previous studies have shown that the deletion of Pfs causes a growth defect in *E. coli* and *E. coli* Δ*pfs* was shown to phenocopy a biotin synthase (*bioB* gene product) mutant [26,27]. The minimal medium M9, which consists of glucose and salts, requires *S.* Typhimurium to generate all the necessary cellular substrates including proteins, carbohydrates and lipids for growth to occur. The *S.* Typhimurium Δ*pfs* mutant was an auxotroph in M9 minimal medium and growth was restored by the provision of Met or biotin. Previous reports have shown that the *E. coli* Δ*pfs* is growth defective in minimal medium and that the addition of Met or biotin partially restored the growth of the *E. coli* Δ*pfs* [26]. Recent findings in other bacteria including *Neisseria meningitides*, *Borrelia burgdorferi* and *Staphylococcus aureus* suggested that Pfs is essential for their virulence [43–45], though the specific mechanism(s) through which attenuation occurs is less clear.

In *S.* Typhimurium Δ*pfs*, the auxotrophic requirement for biotin can be explained by the action of Pfs on 5′-deoxyadenosine, which is both a substrate for Pfs, and a known inhibitor of the biotin synthesis by BioB [27,46]. Why M9 Met auxotrophy was demonstrated by *S.* Typhimurium Δ*pfs* is less clear; subsequent studies revealed that the conversion of SRH to homocysteine, via LuxS, was dispensable suggesting that the activated methyl cycle *per se*, as it is currently modelled, is not essential for the provision of substrates for growth in either minimal medium or in mammalian cells. It may be that the accumulation of SAH is inhibitory for MetK and this inhibition is relieved by increased concentrations of Met. The role of Met in the growth attenuation in HeLa cells was explored through comparing the virulence of the *S.* Typhimurium Δ*pfs* mutant with mutants lacking the major Met importer (MetNIQ), and in *de novo* synthesis through the loss of MetB or MetE/MetH [37], the partially redundant Met synthases. These combined Met mutants did not phenocopy the attenuation observed in the *S.* Typhimurium Δ*pfs* mutant in HeLa cells, suggesting that the inability to produce or scavenge Met was not responsible for the observed *in vivo* growth attenuation. Similarly, since the BioB mutant did not phenocopy the *S.* Typhimurium Δ*pfs*, and the mutants grew like wild-type in HeLa cells and C57BL/6 mice, the attenuation observed in *S.* Typhimurium Δ*pfs* cannot be attributed to a reduction in, or loss of, biotin synthesis.

In addition to methylation, SAM provides a substrate for the synthesis of the polyamines spermidine and spermine [18,23,47–49]. Spermidine synthesis proceeds with the decarboxylation of SAM and is catalysed by SAM decarboxylase (SpeD). Decarboxylated SAM donates an aminopropyl group to putrescine to produce spermidine and MTA, and this reaction is catalysed by SpeE [23,49]. MTA is further converted to MTR by Pfs [23,49]. *E. coli* and *Salmonella* excrete the MTR as these bacteria do not possess a functional Met salvage pathway, due to the lack of a key kinase [41,42,50–53]. The SpeD and SpeE mutants of *S.* Typhimurium had a fully virulent phenotype and were not auxotrophs in M9 minimal medium, suggesting that the absence of these specific polyamines was not growth attenuating, where polyamine transport was intact. We did not examine other polyamines such as putrescine, agmatine or cadaverine. Previous studies have shown that a *S.* Typhimurium polyamine mutant, with deletions of *speB*, *speC*, *speE* and *speF*, showed reduced intracellular growth and replication in epithelial cells and also had reduced competitive fitness compared with the wild-type [54]. Subsequent studies of a SpeE mutant in C57BL/6 mice suggested that loss of *de novo* spermidine synthesis was not grossly attenuating [55]. These collective data suggest that some redundancy for polyamine synthesis may be provided through polyamine transport.

LuxS was not essential for the growth of *S.* Typhimurium in M9 minimal medium, nor for growth in HeLa cells, or in C57BL/6 mice. This observation supports previous studies where *E. coli* and *Salmonella* lacking LuxS did not show any growth defect *in vitro* [56–58]. LuxS plays a potential role in two different aspects of *S.* Typhimurium pathogenesis: in the recycling of Met, and in quorum sensing [12]. Many pathogenic bacteria synthesise LuxS and, in some bacteria, quorum sensing is involved in the control of virulence gene expression, e.g. *Shigella flexneri, Vibrio cholerae*, *Clostridium perfringenes* and *Streptococcus pyogenes* [59–62]. LuxS is also required for meningococcal bacteraemia in mice [63]. In models of the activated methyl cycle in *E. coli* and *Salmonella,* LuxS is required to complete the cycle which can replenish Met from homocysteine. In our study,

Biochemical Journal (2019) 476 3435–3453
https://doi.org/10.1042/BCJ20190297

Met recycling and Met replenishment through LuxS was not essential for *S.* Typhimurium virulence *in vivo*. Also, it was concluded that AI-2 mediated quorum sensing was dispensable for *S.* Typhimurium growth and virulence during systemic infection in highly sensitive mice. These data do not mean that AI-2-mediated quorum sensing is irrelevant to *S.* Typhimurium virulence and it is possible, through effects on community behaviours like swarming motility, that AI-2 provides *S.* Typhimurium a fitness advantage *ex vivo*, which increases transmission efficiency. Indeed, the Pfs mutant lost the swarming phenotype when plated onto soft agar (Supplementary Figure S2).

According to the pathway model (Figure 1), deletion of Pfs should lead to the accumulation of SAH and MTA. Elevated levels of SAH are inhibitory for SAM-dependent methyltransferases [38–40]; similarly, increased concentrations of MTA are inhibitory for polyamine synthases and SAM-dependent methyltransferases [64–67]. Having shown that SpeD, SpeE, LuxS and BioB are dispensable, the hypothesis that SAH accumulation is attenuating was tested through the heterologous expression of SahH, from *Legionella pneumophila*, a SAH hydrolase that lacks MTA nucleosidase activity.

Heterologous expression of *L. pneumophila* SahH (a specific S-adenosylhomocysteine hydrolase) by *S.* Typhimurium Δ*pfs* restored the growth and virulence of this Δ*pfs* mutant in M9 minimal medium, HeLa cells and the murine challenge model, and the complemented mutants reduced the levels of SAH that accumulated in the SL1344 Pfs mutant. The degree of reduction was different but the enzyme kinetics of the two enzymes (*Salmonella* Pfs and *Legionella* SahH) are unknown though in Met-replete M9 medium, there was growth attenuation over the first 18 hr in the Pfs mutant complemented with SahH, compared with Pfs complementation (Supplementary Figure S5). Further Clustal analysis revealed that the *Legionella* SahH and human SahH shared homology, suggesting that *Legionella* may have scavenged SahH from an eukaryotic e.g. the amoebic niche, a theory that has been discussed elsewhere [68,69]. Complementation of growth and virulence by *Legionella* SahH suggests that suppression of the SAM-dependent methyltransferases by SAH may be responsible for the attenuation observed in *S.* Typhimurium Δ*pfs*. However, analysis of the DNA from *S.* Typhimurium Δ*pfs* suggested that DNA methylation was unaffected at the gross level. This could mean that essential methylases targeting other functions were affected by accumulated SAH. *S.* Typhimurium carries a number of proteins with potential SAM-binding motifs [70], such as PmtA, a phospholipid N-methyl transferase required for membrane synthesis, the expression of which may be repressed by higher levels of SAH.

In summary, these studies suggest that the multifunctional enzyme Pfs may be a legitimate antibiotic target. While the auxotrophy in minimal medium can be alleviated by biotin or Met, the relationship between the availability of these substrates, and the severe attenuation observed in murine infections, is yet to be resolved. Clustal analysis of the *E. coli* and *Salmonella* spp. Pfs revealed significant homology, which was absent from the *L. pneumophila* SahH. *S.* Typhimurium lacking Pfs shows severe growth attenuation in highly sensitive mice, and this growth inhibition appears to be due to the accumulation of the metabolite SAH. While the SahH enzyme from *Legionella pneumophila* shares significant homology with the human enzyme, Similarity Network Analysis revealed that many bacterial Pfs genes form a separate and distinct family of proteins, suggesting that it may be possible to generate inhibitors specific for bacterial enaymes, which leave mammalian enzymes unaffected and to effect selective toxicity.

Abbreviations

AI-2, autoinducer-2; cfu, colony-forming units; FCS, fetal calf serum; Met, methionine; MTA, methylthioadenosine; MTR, methylthioribose; *S*. Typhimurium, *Salmonella enterica* var Typhimurium; SAH, S-adenosylhomocysteine; SAH/MTA, S-adenosylhomocysteine/Methylthioadenosine; SAM, S-adenosylmethionine.

Author Contributions

A.U.H. perfomed experiments, generated mutants and helped write the paper, N.W. performed animal experiments and helped write the paper, J.J.W. constructed some key mutants and helped write the paper, H.J. N. designed and helped interpret key *in vitro* experiments, S.A.C. and D.M.H. provided key data and helped write the paper, I.D.H. generated key figures explaining the relationships between the various enzymes, M.R.D. performed bioinformatic analysis of key genes, M.J.M. helped design experiments and provided key insights into metabolic processes and helped write the paper, T.L. provided key insights into enzyme family relationships and helped write the paper, R.A.S. designed key experiments and helped write the paper.

Funding

The authors acknowledge the support of the National Health and Medical Research Council in providing a Program Grant to TL and RAS (APP1092262) and an Australian Research Council Laureate Fellowship in support of TL (FL130100038).

Competing Interests

The authors declare that there are no competing interests associated with the manuscript.

References

1 Coates, A. and Hu, Y. (2007) Novel approaches to developing new antibiotics for bacterial infections. *Br. J. Pharmacol.* **152**, 1147–1154 https://doi.org/10.1038/sj.bjp.0707432
2 Harada, E., Iida, K.-I., Shiota, S., Nakayama, H. and Yoshida, S.-I. (2010) Glucose metabolism in *Legionella pneumophila*: dependence on the Entner-Doudoroff pathway and connection with intracellular bacterial growth. *J. Bacteriol.* **192**, 2892–2899 https://doi.org/10.1128/JB.01535-09
3 Rossi, M., Amaretti, A. and Raimondi, S. (2011) Folate production by probiotic bacteria. *Nutrients* **3**, 118–134 https://doi.org/10.3390/nu3010118
4 Pitchandi, P., Hopper, W. and Rao, R. (2013) Comprehensive database of Chorismate synthase enzyme from shikimate pathway in pathogenic bacteria. *BMC Pharmacol. Toxicol.* **14**, 29 https://doi.org/10.1186/2050-6511-14-29
5 Bourne, C.R. (2014) Utility of the biosynthetic folate pathway for targets in antimicrobial discovery. *Antibiotics* **3**, 1–28 https://doi.org/10.3390/antibiotics3010001
6 Walsh, C. (2003) Where will new antibiotics come from? *Nat. Rev. Microbiol.* **1**, 65–70 https://doi.org/10.1038/nrmicro727
7 Muñoz-Elías, E.J. and McKinney, J.D. (2006) Carbon metabolism of intracellular bacteria. *Cell. Microbiol.* **8**, 10–22 https://doi.org/10.1111/j.1462-5822.2005.00648.x
8 Murima, P., McKinney, J.D. and Pethe, K. (2014) Targeting bacterial central metabolism for drug development. *Chem. Biol.* **21**, 1423–1432 https://doi.org/10.1016/j.chembiol.2014.08.020
9 Schauder, S. and Bassler, B.L. (2001) The languages of bacteria. *Genes Dev.* **15**, 1468–1480 https://doi.org/10.1101/gad.899601
10 Winzer, K., Hardie, K.R., Burgess, N., Doherty, N., Kirke, D., Holden, M.T. et al. (2002) Luxs: its role in central metabolism and the in vitro synthesis of 4-hydroxy-5-methyl-3 (2H)-furanone. *Microbiology* **148**, 909–922 https://doi.org/10.1099/00221287-148-4-909
11 Xavier, K.B. and Bassler, B.L. (2003) Luxs quorum sensing: more than just a numbers game. *Curr. Opin. Microbiol.* **6**, 191–197 https://doi.org/10.1016/S1369-5274(03)00028-6
12 Vendeville, A., Winzer, K., Heurlier, K., Tang, C.M. and Hardie, K.R. (2005) Making'sense' of metabolism: autoinducer-2, LuxS and pathogenic bacteria. *Nat. Rev. Microbiol.* **3**, 383–396 https://doi.org/10.1038/nrmicro1146
13 Choi, J., Shin, D. and Ryu, S. (2007) Implication of quorum sensing in *Salmonella enterica* serovar typhimurium virulence: the luxS gene is necessary for expression of genes in pathogenicity island 1. *Infect. Immun.* **75**, 4885–4890 https://doi.org/10.1128/IAI.01942-06
14 Beeston, A.L. (2002) Surette MG. pfs-dependent regulation of autoinducer 2 production in *Salmonella enterica* serovar *Typhimurium*. *J. Bacteriol.* **184**, 3450–3456 https://doi.org/10.1128/JB.184.13.3450-3456.2002
15 Miller, M.B. and Bassler, B.L. (2001) Quorum sensing in bacteria. *Annu. Rev. Microbiol.* **55**, 165–199 https://doi.org/10.1146/annurev.micro.55.1.165
16 Kimchi, B. and Ron, E.Z. (1987) A mutant of *Escherichia coli* temperature sensitive in the biosynthesis of S-adenosylmethionine. *FEMS Microbiol. Lett.* **43**, 101–106 https://doi.org/10.1111/j.1574-6968.1987.tb02105.x
17 Satishchandran, C., Taylor, J. and Markham, G. (1990) Novel *Escherichia coli* K-12 mutants impaired in *S*-adenosylmethionine synthesis. *J. Bacteriol.* **172**, 4489–4496 https://doi.org/10.1128/jb.172.8.4489-4496.1990
18 Chiang, P., Gordon, R.K., Tal, J., Zeng, G., Doctor, B., Pardhasaradhi, K. et al. (1996) *S*-adenosylmethionine and methylation. *FASEB J.* **10**, 471–480 https://doi.org/10.1096/fasebj.10.4.8647346
19 Fontecave, M., Atta, M. and Mulliez, E. (2004) S-adenosylmethionine: nothing goes to waste. *Trends Biochem. Sci.* **29**, 243–249 https://doi.org/10.1016/j.tibs.2004.03.007
20 Wei, Y. and Newman, E. (2002) Studies on the role of the metK gene product of *Escherichia coli* K-12. *Mol. Microbiol.* **43**, 1651–1656 https://doi.org/10.1046/j.1365-2958.2002.02856.x
21 Struck, A.W., Thompson, M.L., Wong, L.S. and Micklefield, J. (2012) S-adenosyl-methionine-dependent methyltransferases: highly versatile enzymes in biocatalysis, biosynthesis and other biotechnological applications. *ChemBioChem* **13**, 2642–2655 https://doi.org/10.1002/cbic.201200556
22 Parveen, N. and Cornell, K.A. (2011) Methylthioadenosine/S-adenosylhomocysteine nucleosidase, a critical enzyme for bacterial metabolism. *Mol. Microbiol.* **79**, 7–20 https://doi.org/10.1111/j.1365-2958.2010.07455.x
23 Kanehisa, M., Sato, Y., Kawashima, M., Furumichi, M. and Tanabe, M. (2015) KEGG as a reference resource for gene and protein annotation. *Nucleic Acids Res.* **44**, D457–DD62 https://doi.org/10.1093/nar/gkv1070
24 Duerre, J., Walker, R., Salvatore, F., Borek, E., Zappia, V., Williams-Ashman, H. et al. (1977) *The Biochemistry of Adenosylmethionine*, Columbia University Press, New York
25 Turner, M.A., Yang, X., Yin, D., Kuczera, K., Borchardt, R.T. and Howell, P.L. (2000) Structure and function of S-adenosylhomocysteine hydrolase. *Cell Biochem. Biophys.* **33**, 101–125 https://doi.org/10.1385/CBB:33:2:101
26 Cadieux, N., Bradbeer, C., Reeger-Schneider, E., Köster, W., Mohanty, A.K., Wiener, M.C. et al. (2002) Identification of the periplasmic cobalamin-binding protein BtuF of *Escherichia coli*. *J. Bacteriol.* **184**, 706–717 https://doi.org/10.1128/JB.184.3.706-717.2002
27 Choi-Rhee, E. and Cronan, J.E. (2005) A nucleosidase required for in vivo function of the S-adenosyl-L-methionine radical enzyme, biotin synthase. *Chem. Biol.* **12**, 589–593 https://doi.org/10.1016/j.chembiol.2005.04.012
28 Hoiseth, S.K. and Stocker, B.A. (1981) Aromatic-dependent *Salmonella typhimurium* are non-virulent and effective as live vaccines. *Nature* **291**, 238–239 https://doi.org/10.1038/291238a0
29 Herring, C.D., Glasner, J.D. and Blattner, F.R. (2003) Gene replacement without selection: regulated suppression of amber mutations in *Escherichia coli*. *Gene* **311**, 153–163 https://doi.org/10.1016/S0378-1119(03)00585-7

Biochemical Journal (2019) **476** 3435–3453
https://doi.org/10.1042/BCJ20190297

30 Davis, R.W., Botstein, D. and Roth, J.R. (1980) *Advanced Bacterial Genetics*, Cold Spring Harbor Laboratory
31 Mandell, G.L. (1973) Interaction of intraleukocytic bacteria and antibiotics. *J. Clin. Invest.* **52**, 1673–1679 https://doi.org/10.1172/JCI107348
32 Vaudaux, P. and Waldvogel, F.A. (1979) Gentamicin antibacterial activity in the presence of human polymorphonuclear leukocytes. *Antimicrob. Agents Chemother.* **16**, 743–749 https://doi.org/10.1128/AAC.16.6.743
33 Cobbold, S.A. and McConville, M.J. (2019) Determining the mode of action of antimalarial drugs using time-resolved LC–MS-based metabolite profiling. *Methods Mol. Biol.* **1859**, 225–239 https://doi.org/10.1007/978-1-4939-8757-3_12
34 Clasquin, M.F., Melamud, E. and Rabinowitz, J.D. (2012) LC–MS data processing with MAVEN: a metabolomic analysis and visualization engine. *Curr. Protoc. Bioinformatics* **37**, 14.1.1–14.1.23 https://doi.org/10.1002/0471250953.bi1411s37
35 Frickey, T. and Lupas, A. (2004) CLANS: a Java application for visualizing protein families based on pairwise similarity. *Bioinformatics* **20**, 3702–3704 https://doi.org/10.1093/bioinformatics/bth444
36 Strugnell, R.A., Scott, T.A., Wang, N., Yang, C., Peres, N., Bedoui, S. et al. (2014) Salmonella vaccines: lessons from the mouse model or bad teaching? *Curr. Opin. Microbiol.* **17**, 99–105 https://doi.org/10.1016/j.mib.2013.12.004
37 Husna, A.U., Wang, N., Cobbold, S.A., Newton, H.J., Hocking, D.M., Wilksch, J.J. et al. (2018) Methionine biosynthesis and transport are functionally redundant for the growth and virulence of *Salmonella Typhimurium*. *J. Biol. Chem.* **293**, 9506–9519 https://doi.org/10.1074/jbc.RA118.002592
38 Reich, N. and Mashhoon, N. (1990) Inhibition of EcoRI DNA methylase with cofactor analogs. *J. Biol. Chem.* **265**, 8966–8970 PMID:2341414
39 Reich, N.O. and Mashhoon, N. (1991) Kinetic mechanism of the EcoRI DNA methyltransferase. *Biochemistry* **30**, 2933–2939 https://doi.org/10.1021/bi00225a029
40 Simms, S. and Subbaramaiah, K. (1991) The kinetic mechanism of S-adenosyl-L-methionine: glutamylmethyltransferase from *Salmonella typhimurium*. *J. Biol. Chem.* **266**, 12741–6 PMID:2061337
41 Sekowska, A., Dénervaud, V., Ashida, H., Michoud, K., Haas, D., Yokota, A. et al. (2004) Bacterial variations on the methionine salvage pathway. *BMC Microbiol.* **4**, 9 https://doi.org/10.1186/1471-2180-4-9
42 Sekowska, A., Kung, H.-F. and Danchin, A. (2000) Sulfur metabolism in *Escherichia coli* and related bacteria: facts and fiction. *J. Mol. Microbiol. Biotechnol.* **2**, 145–177 PMID:10939241
43 Heurlier, K., Vendeville, A., Halliday, N., Green, A., Winzer, K., Tang, C.M. et al. (2009) Growth deficiencies of *Neisseria meningitidis* pfs and luxS mutants are not due to inactivation of quorum sensing. *J. Bacteriol.* **191**, 1293–1302 https://doi.org/10.1128/JB.01170-08
44 Cornell, K.A., Primus, S., Martinez, J.A. and Parveen, N. (2009) Assessment of methylthioadenosine/S-adenosylhomocysteine nucleosidases of *Borrelia burgdorferi* as targets for novel antimicrobials using a novel high-throughput method. *J. Antimicrob. Chemother.* **63**, 1163–1172 https://doi.org/10.1093/jac/dkp129
45 Bao, Y., Li, Y., Jiang, Q., Zhao, L., Xue, T., Hu, B. et al. (2013) Methylthioadenosine/S-adenosylhomocysteine nucleosidase (Pfs) of *Staphylococcus aureus* is essential for the virulence independent of LuxS/AI-2 system. *Int. J. Med. Microbiol.* **303**, 190–200 https://doi.org/10.1016/j.ijmm.2013.03.004
46 Ollagnier-de-Choudens, S., Mulliez, E. and Fontecave, M. (2002) The PLP-dependent biotin synthase from *Escherichia coli*: mechanistic studies. *FEBS Lett.* **532**, 465–468 https://doi.org/10.1016/S0014-5793(02)03733-X
47 Bowman, W.H., Tabor, C.W. and Tabor, H. (1973) Spermidine biosynthesis purification and properties of propylamine transferase from *Escherichia coli*. *J. Biol. Chem.* **248**, 2480–2486 PMID:4572733
48 Salvatore, F., Borek, E., Zappia, V., Williams-Ashman, H.G. and Schlenk, F. (eds.) (1977) The Biochemistry of Adenosylmethionine. Columbia University Press, New York, USA
49 Shah, P. and Swiatlo, E. (2008) A multifaceted role for polyamines in bacterial pathogens. *Mol. Microbiol.* **68**, 4–16 https://doi.org/10.1111/j.1365-2958.2008.06126.x
50 Schroeder, H.R., Barnes, C., Bohinski, R. and Mallette, M. (1973) Biological production of 5-methylthioribose. *Can. J. Microbiol.* **19**, 1347–1354 https://doi.org/10.1139/m73-217
51 Hughes, J.A. (2006) In vivo hydrolysis of S-adenosyl-L-methionine in *Escherichia coli* increases export of 5-methylthioribose. *Can. J. Microbiol.* **52**, 599–602 https://doi.org/10.1139/w06-008
52 Albers, E. (2009) Metabolic characteristics and importance of the universal methionine salvage pathway recycling methionine from 5′-methylthioadenosine. *IUBMB Life* **61**, 1132–1142 https://doi.org/10.1002/iub.278
53 Mackie, A., Keseler, I.M., Nolan, L., Karp, P.D. and Paulsen, I.T. (2013) Dead end metabolites-defining the known unknowns of the *E. coli* metabolic network. *PLoS ONE* **8**, e75210 https://doi.org/10.1371/journal.pone.0075210
54 Jelsbak, L., Thomsen, L.E., Wallrodt, I., Jensen, P.R. and Olsen, J.E. (2012) Polyamines are required for virulence in *Salmonella enterica* serovar *Typhimurium*. *PLoS ONE* **7**, e36149 https://doi.org/10.1371/journal.pone.0036149
55 Espinel, I.C., Guerra, P.R. and Jelsbak, L. (2016) Multiple roles of putrescine and spermidine in stress resistance and virulence of *Salmonella enterica* serovar *Typhimurium*. *Microb. Pathog.* **95**, 117–123 https://doi.org/10.1016/j.micpath.2016.03.008
56 Sperandio, V., Torres, A.G., Girón, J.A. and Kaper, J.B. (2001) Quorum sensing is a global regulatory mechanism in enterohemorrhagic *Escherichia coli* O157: H7. *J. Bacteriol.* **183**, 5187–5197 https://doi.org/10.1128/JB.183.17.5187-5197.2001
57 Taga, M.E., Miller, S.T. and Bassler, B.L. (2003) Lsr-mediated transport and processing of AI-2 in *Salmonella typhimurium*. *Mol. Microbiol.* **50**, 1411–1427 https://doi.org/10.1046/j.1365-2958.2003.03781.x
58 Wang, L., Li, J., March, J.C., Valdes, J.J. and Bentley, W.E. (2005) luxS-dependent gene regulation in *Escherichia coli* K-12 revealed by genomic expression profiling. *J. Bacteriol.* **187**, 8350–8360 https://doi.org/10.1128/JB.187.24.8350-8360.2005
59 Day, W.A. and Maurelli, A.T. (2001) *Shigella flexneri* LuxS quorum-sensing system modulates virB expression but is not essential for virulence. *Infect. Immun.* **69**, 15–23 https://doi.org/10.1128/IAI.69.1.15-23.2001
60 Zhu, J., Miller, M.B., Vance, R.E., Dziejman, M., Bassler, B.L. and Mekalanos, J.J. (2002) Quorum-sensing regulators control virulence gene expression in *Vibrio cholerae*. *Proc. Natl Acad. Sci. U.S.A.* **99**, 3129–3134 https://doi.org/10.1073/pnas.052694299
61 Ohtani, K., Hayashi, H. and Shimizu, T. (2002) The luxS gene is involved in cell–cell signalling for toxin production in *Clostridium* perfringens. *Mol. Microbiol.* **44**, 171–179 https://doi.org/10.1046/j.1365-2958.2002.02863.x
62 Siller, M., Janapatla, R.P., Pirzada, Z.A., Hassler, C., Zinkl, D. and Charpentier, E. (2008) Functional analysis of the group A streptococcal luxS/AI-2 system in metabolism, adaptation to stress and interaction with host cells. *BMC Microbiol.* **8**, 1 https://doi.org/10.1186/1471-2180-8-188

63 Winzer, K., Sun, Y.-H., Green, A., Delory, M., Blackley, D., Hardie, K.R. et al. (2002) Role of *Neisseria meningitidis* luxS in cell-to-cell signaling and bacteremic infection. *Infect. Immun.* **70**, 2245–2248 https://doi.org/10.1128/IAI.70.4.2245-2248.2002
64 Pajula, R.-L. (1983) Kinetic properties of spermine synthase from bovine brain. *Biochem. J.* **215**, 669–676 https://doi.org/10.1042/bj2150669
65 Pajula, R.-L. and Raina, A. (1979) Methylthioadenosine, a potent inhibitor of spermine synthase from bovine brain. *FEBS Lett.* **99**, 343–345 https://doi.org/10.1016/0014-5793(79)80988-6
66 Christa, L., Kersual, J., Auge, J. and Perignon, J.-L. (1988) Methylthioadenosine toxicity and metabolism to methionine in mammalian cells. *Biochem. J.* **255**, 145–152 https://doi.org/10.1042/bj2550145
67 Galletti, P., Oliva, A., Manna, C., Della Ragione, F. and Cartenì-Farina, M. (1981) Effect of 5′-methylthioadenosine on in vivo methyl esterification of human erythrocyte membrane proteins. *FEBS Lett.* **126**, 236–240 https://doi.org/10.1016/0014-5793(81)80250-5
68 Cohan, F.M. and Koeppel, A.F. (2008) The origins of ecological diversity in prokaryotes. *Curr. Biol.* **18**, R1024–R1R34 https://doi.org/10.1016/j.cub.2008.09.014
69 Wiedenbeck, J. and Cohan, F.M. (2011) Origins of bacterial diversity through horizontal genetic transfer and adaptation to new ecological niches. *FEMS Microbiol. Rev.* **35**, 957–976 https://doi.org/10.1111/j.1574-6976.2011.00292.x
70 Aktas, M., Gleichenhagen, J., Stoll, R. and Narberhaus, F. (2011) S-adenosylmethionine-binding properties of a bacterial phospholipid N-methyltransferase. *J. Bacteriol.* **193**, 3473–3481 https://doi.org/10.1128/JB.01539-10
71 Turner, S., Carbone, F. and Strugnell, R. (1993) *Salmonella typhimurium* delta aroA delta aroD mutants expressing a foreign recombinant protein induce specific major histocompatibility complex class I-restricted cytotoxic T lymphocytes in mice. *Infect. Immun.* **61**, 5374–5380 PMID:8225611
72 Grant, S.G., Jessee, J., Bloom, F.R. and Hanahan, D. (1990) Differential plasmid rescue from transgenic mouse DNAs into *Escherichia coli* methylation-restriction mutants. *Proc. Natl Acad. Sci. U.S.A.* **87**, 4645–4649 https://doi.org/10.1073/pnas.87.12.4645
73 Chang, A.C. and Cohen, S.N. (1978) Construction and characterization of amplifiable multicopy DNA cloning vehicles derived from the P15A cryptic miniplasmid. *J. Bacteriol.* **134**, 1141–1156 PMID:149110
74 Cherepanov, P.P. and Wackernagel, W. (1995) Gene disruption in *Escherichia coli*: Tc R and Km R cassettes with the option of Flp-catalyzed excision of the antibiotic-resistance determinant. *Gene* **158**, 9–14 https://doi.org/10.1016/0378-1119(95)00193-A
75 Datsenko, K.A. and Wanner, B.L. (2000) One-step inactivation of chromosomal genes in *Escherichia coli* K-12 using PCR products. *Proc. Natl Acad. Sci. U.S.A.* **97**, 6640–6645 https://doi.org/10.1073/pnas.120163297